THERMAL MAGNETORESISTANCE

The array of sophisticated experimental techniques available to solid-state researchers and device engineers for exploring the physical properties and the device potential of materials is truly impressive, and the development of new, specialized probes shows no signs of abating. This article focuses on the methods and techniques of thermal magnetoresistance in solids containing magnetic constituents. Although a rather specialized topic, thermal magnetoresistance is of considerable relevance to several classes of magnetic and superconducting materials that have recently generated much excitement in the scientific community for their unusual magnetic properties. Some of these materials, notably the magnetic multilayers and the manganite perovskites, have gained rapid acceptance as the materials of choice for magnetooptic recording technology.

As the term *thermal magnetoresistance* implies, the phenomenon has its foundation in the flow of heat through a solid and in how this thermal current is influenced by an externally applied magnetic field. Thermal magnetoresistance effects are closely related to the more familiar magnetoresistance effects caused by an external magnetic field acting on an electrical current. Within ordinary semiconductors or nonmagnetic metals both magnetoresistance and thermal magnetoresistance (often referred to as the Righi–Leduc effect) are well-understood transport effects that arise as a consequence of the Lorentz force acting on a moving charge in the presence of a transverse magnetic field. Semiconductor and semimetal-based magnetoresistors and Hall-effect devices are widely used as detectors of a magnetic field and its strength, and as position and motion sensors. They are adequately described in the literature and they are not considered in this article.

The focus here is on changes in thermal and electric currents brought about by manipulation of the magnetic state of a sample—for example, as the external magnetic field is ramped up from zero to some predetermined value. Thus it is important to keep in mind that only solids that contain some kind of magnetic structure will be considered here; it is the orientation of the sample's magnetization that determines how efficiently heat or an electric current will flow in such solids. The goal is to change the orientation of magnetization in order to modulate the heat current.

Specifically, three distinct situations in which the effect of a magnetic field leads to a dramatic change in a material's ability to conduct heat will be considered. First, thermal magnetoresistance in magnetic multilayer films and granular structures that display the so-called giant magnetoresistance (GMR) effect; second, thermal magnetoresistance in the mixed-valent state of manganite perovskites that exhibit extremely large magnetoresistance, referred to as colossal magnetoresistance (CMR), will be discussed. Finally, thermal magnetoresistance in the mixed state of high-temperature superconductors, where magnetic vortices strongly influence heat transport, will be discussed. One class of solids that displays significant thermal magnetoresistance and that is not covered in this article is crystals containing paramagnetic ions. The reader is referred to a review article by Smirnov and Oskotski (1) where these solids are described in detail. Before engaging in a detailed discussion of thermal magnetoresistance in the above three systems, it will be helpful to recall some fundamental points underlying heat transport in solids and to remember the basic notions concerning magnetically ordered structures.

HEAT CONDUCTION IN SOLIDS

One of the most important questions a design engineer must consider when drawing plans for a new electronic structure is how efficiently it can carry and distribute heat. Heat, both in its beneficial form and as an undesirable by-product of power dissipation, is all around us, and the challenge is to be able to distribute it, to convert it and, in general, to manage it so that the device operates within its temperature tolerance. The physical quantity that reflects how efficiently a given material conducts heat is called the material's thermal conductivity. The range of values of thermal conductivity in solids spans some five decades of magnitude, from very poor heat conductors represented by porous materials, plastics, and glasses, to solids, with an outstanding ability to conduct heat, such as copper, silver, and diamond.

Thermal conductivity of a material is not only an important empirical parameter of obvious technological relevance, but also a powerful experimental probe of the structural and transport properties of matter. Quantum theoretical treatment of these thermal transport processes, combined with a detailed understanding of defect structures and scattering processes, has reached a level of sophistication that now allows for reliable qualitative predictions of temperature-dependent behavior and sometimes even good quantitative estimates of thermal conductivity. In some instances, such as in the case of heat transport in diamonds, the sensitivity of thermal conductivity to structural imperfections rivals that of the most sophisticated spectroscopic techniques. In general, thermal conductivity measurements have been invaluable in assessing the constituency and character of the thermal transport processes, providing information about the electronic and vibrational properties of materials, shedding light on the dominant interactions within solids, and—in a nondestructive way—giving insight into the defect structure of materials.

According to Fourier's law, the thermal gradient, ∇T, imposed across a block of an isotropic solid results in a heat flow rate Q—across a cross-section of area A perpendicular to the direction of the heat flow—that is given by

$$Q = -\kappa A \nabla T \tag{1}$$

The thermal conductivity, κ, reflects how efficiently the material carries heat, and the negative sign signifies that heat flows down the thermal gradient—that is, from the warmer to the colder face of the block as required by the second law of thermodynamics. In practice, rather than measuring the gradient, ∇T, one measures the temperature difference, $\Delta T = T_{\mathrm{hot}} - T_{\mathrm{cold}}$, between two points separated by a distance L along the direction of heat flow. In this case, Eq. (2) serves both as a definition of the thermal conductivity and as a practical means of its empirical determination:

$$\kappa = -\frac{Q}{A\nabla T} = \frac{Q}{\Delta T}\frac{L}{A} \tag{2}$$

Two entities dominate heat flow in a solid: (1) free carriers (electrons and their positively charged counterparts, called holes) contributing the term known as electronic (or carrier) thermal conductivity, κ_e; and (2) quantized lattice vibrations called phonons that yield the phonon (or lattice) thermal conductivity, κ_p. To a first approximation, they act as independent heat-conducting channels and the total thermal conductivity is equal to

$$\kappa = \kappa_e + \kappa_p \tag{3}$$

While the phonon thermal conductivity, κ_p, is present in all solids, the magnitude of the electronic contribution depends on the type of material under consideration. Thus, κ_e is zero in insulators, is small or comparable to the phonon contribution in semiconductors (depending on the level of doping), and is overwhelmingly dominant in heat transport in metals. In superconductors, both κ_p and κ_e are expected to contribute to the thermal conductivity. Since conventional superconductors have a high free-carrier density, κ_e usually dominates. In high-temperature superconductors, where the Hall effect and other experimental evidence suggests a significant reduction in the carrier density, the relative weight of the two thermal conductivity terms shifts in favor of the phonon contribution, κ_p. Below the superconducting transition temperature, however, both phonons and quasiparticles ("normal"-like excitations of a superconductor) contribute to the flow of heat.

Charge carrier populations and phonon populations both are specified by their distribution functions and the corresponding densities of state. Electrons are fermions (particles with noninteger spin—in this case spin of 1/2) and are described by the well-known Fermi–Dirac distribution function:

$$f(E) = \frac{1}{e^{(E-E_F)/k_B T} + 1} \tag{4}$$

where $f(E)$ is the probability of a state of energy E being occupied, E_F is the Fermi energy, and k_B is the Boltzmann constant. Phonons, on the other hand, are bosons—particles with a spin of zero—and they obey the Bose–Einstein statistics with the distribution function

$$N(\omega) = \frac{1}{e^{\hbar\omega/k_BT} - 1} \tag{5}$$

Here $N(\omega)$ is the average number of phonons associated with the normal mode of frequency ω at temperature T, and $\hbar = h/2\pi$, where h is the Planck constant. It is important to realize that equilibrium distributions of charge carriers and phonons do not lead to the transport of thermal energy. It is only when these distributions are perturbed by an externally imposed thermal gradient that heat can flow in a solid. To prevent a runaway of heat, the charge carrier and phonon distributions must be relaxed—that is, the carriers and phonons must participate in the scattering processes that tend to restore equilibrium. The net effect is the establishment of steady-state nonequilibrium distribution accompanied by the resulting heat flow. For each scattering process one can introduce a relaxation time, τ_i, as the average time that elapses before the perturbed distribution function returns to equilibrium. According to Matthiessen's rule, the scattering processes—that is, heat resistivities—within each channel are additive. The overall behavior of the thermal conductivity then reflects the strength of the scattering processes and their temperature dependence. Scattering cross-sections for essentially every conceivable interaction of charge carriers and phonons have been worked out using the techniques of quantum and statistical mechanics and are available in the literature, for example, Klemens (2).

Thermal conductivity is often discussed in terms of the magnitude of the mean-free path of the heat carrying entities—electrons, ℓ_e, and phonons, ℓ_p. The mean-free path here is understood as some average distance the charge carrier or phonon travels before it gives up its excess of thermal energy in collisions within the solid. With the aid of the mean-free path, and knowing the specific heat, C, and the average velocity of the charge carriers, v, (or the speed of sound, in the case of phonons), one can invoke kinetic theory to write the thermal conductivity in the form

$$\kappa = \frac{1}{3} C v \ell \tag{6}$$

Equation (6) is a convenient form for writing the thermal conductivity for the electronic contribution, κ_e, as well as for the phonon thermal conductivity, κ_p. Of course, summing over all possible phonon modes and their polarizations, as well as adding all carrier species that may participate in the transport, is necessary if Eq. (6) is to be made a realistic representation of thermal conductivity.

Since the charge carriers transport not just the charge but also heat (excess of the thermal energy given by the Fermi distribution function), it is not surprising that the carrier thermal conductivity, κ_e, is related to the electrical conductivity, σ, or to its inverse, the electrical resistivity, ρ. Based on empirical evidence in metals, this interdependence has been known to exist since the middle of the last century and is referred to as the Wiedemann–Franz law:

$$\kappa_e = \sigma L_0 T = \frac{L_0 T}{\rho} \tag{7}$$

Here L_0 is the Lorenz number. Treating electrons as a highly degenerate system and using methods of quantum statistical mechanics, gives the Lorenz number as

$$L_0 = \frac{\pi^2}{3}\left(\frac{k_B}{e}\right)^2 = 2.45 \times 10^{-8} V^2 K^{-2} \tag{8}$$

For the Wiedemann–Franz law to be valid it necessarily means that the nonequilibrium carrier distributions generated by the electric field and by the thermal gradient must relax to the state of thermal equilibrium at the same rate. The question is, under what conditions does this really happen?

Rather than providing a lengthy and tedious mathematical treatment [e.g., Ziman (3)], the essential physics have been captured in Fig. 1, where distribution functions for a degenerate gas of electrons are sketched. Figure 1(a) illustrates the departure from equilibrium due to an electric field, while Fig. 1(b) depicts the deviation from equilibrium due to a thermal gradient. The solid curves represent the equilibrium distributions, while the dashed curves correspond to the perturbed distributions. In both cases the deviations from equilibrium are significant only near the Fermi surface, marked as E_F, because only electrons within the energy range of k_BT near E_F can respond to external stimuli such as an electric field or a thermal gradient. Electrons deep inside the distribution, being governed by the Pauli exclusion principle, cannot move from their energy levels because all neighboring states are occupied and no two electrons (neglecting spin) can share the same energy level.

The effect of an electric field is to displace the entire distribution to the right but leave its shape intact (provided the relaxation time of all electrons near the Fermi surface is the same). This means that the energy levels previously unoccu-

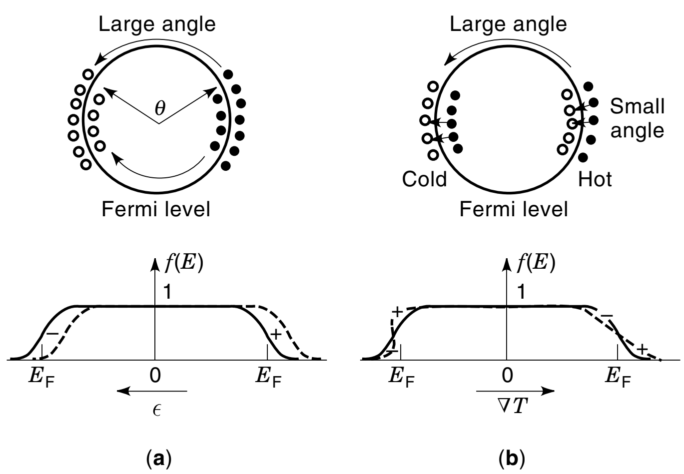

Figure 1. Schematic representation of the undisturbed (solid curves) and disturbed (dashed curves) Fermi distributions produced by (a) an electric field, and (b) a temperature gradient. The overpopulated and underpopulated energy levels are marked with the + and - signs, respectively. Solid and open circles in the upper panels represent the excess and deficiency of electrons relative to equilibrium distribution. It should be pointed out that an electric field shifts the entire distribution while a temperature gradient creates asymmetry in the distribution function. The reader should note the distinction between the large-angle scattering and small-angle scattering.

pied on the right-hand side are now filled (marked as +) and the levels on the left-hand side of the picture, previously occupied, are now underpopulated (marked −). Scattering processes will tend to restore the equilibrium and they will do so on average in the time τ by taking electrons from the regions marked + and moving them all the way around to the regions marked −. Thus, for the electrons to relax, they must undergo large-angle scattering (and thus large change in their momentum), but in such a way that their energy is not changed. This is referred to as large-angle elastic scattering.

Since thermal conductivity is always measured assuming that no electric current flows, diffusing electrons from the hot end of the sample (where they have a somewhat larger thermal energy) must necessarily be counterbalanced by the flow of colder electrons moving from the cold end of the sample. This leads to a deviation in the distribution function depicted in Fig. 1(b). Electrons traveling down the temperature gradient, that is, in the direction of $-\nabla T$, are "hotter" because their last thermalizing collision was at a point where the temperature was higher. They are thus excited from below to above E_F and, in the process, they spread the distribution on the right-hand side of Fig. 1(b). In contrast, electrons traveling up the thermal gradient are "colder" and they tend to sharpen the distribution as more of them condense below E_F and fewer are excited above E_F. It is immediately obvious that the two distribution functions in Figs. 1(a) and 1(b) are significantly different and it is therefore likely that they will relax in different ways. While it is possible to relax the thermally driven distribution by scattering the hot electrons from the region marked + on the right-hand side of Fig. 1(b) through large angles all the way to the regions marked − on the left-hand side of the figure—that is, relying on the same large-angle elastic process that was effective in relaxing the electric field-produced distribution in Fig. 1(a)—there is another way to relax the thermal nonequilibrium in Fig. 1(b). The electrons can be scattered through very small angles and suffer a small energy change as they move across the Fermi surface—that is, electrons from the + regions on the right-hand side of Fig. 1(b) fill the empty states on the right, and the underpopulated regions on the left-hand side are filled by electrons from below the Fermi surface on the left. Thus there is an additional resistive process for thermal conductivity. The essential point is that if scattering is elastic—that is, if energy is kept constant during the process—both thermal and electrical conductivity will be affected equally and the same relaxation time will apply to both. However, if scattering is inelastic, small-angle scattering may not have much effect on the electrical conductivity but it may very effectively degrade thermal conductivity and, in the process, lead to significant departures from the Wiedemann–Franz law.

In spite of the inelastic nature of electron–phonon scattering, there are always plenty of large wave–vector phonons available at an ambient temperature, and they can effectively relax both electrical and thermal nonequilibrium distributions, and thus the Wiedemann–Franz law applies. At very low temperatures, the dominant resistive process is impurity scattering, which is an elastic process. Hence, the Wiedemann–Franz law holds also at low temperatures. Difficulties arise at intermediate temperatures, where electrons are scattered predominantly by phonons and undergo changes in energy on the order of k_BT. At the same time, there are now not enough large wave–vector phonons available to relax the electrical conductivity in a single collision. While the predominating small wave–vector phonons are very effective in relaxing thermal conductivity (they allow the hot electrons to dump their excess energy by crossing the Fermi surface), one needs many such small wave–vector phonon processes to relax the electrical conductivity. This is what causes the two relaxation times to differ and why the Wiedemann–Franz law is violated. In situations where the Wiedemann–Franz law applies, Eq. (7) allows one to calculate the carrier thermal conductivity, κ_e, from the values of the electrical resistivity, and Eq. (3) can be used to separate the total thermal conductivity into its carrier and phonon contributions.

In a perfect crystal with a potential that is a purely quadratic (harmonic) function of atomic displacements, the lattice excitations would propagate independently and would lack any mutual interactions. Such a distribution of phonons would be impossible to relax and the thermal conductivity would be infinite. What makes the thermal conductivity of solids (even of perfect crystals) finite is the fact that the potential is not strictly harmonic. After all, solids do expand and contract, a clear sign of the presence of anharmonic terms in the lattice potential. Anharmonicity of the lattice facilitates interactions among the normal modes. A simplest form of anharmonicity which includes only a cubic term in the potential brings into focus three-phonon processes for which the transition probability is essentially zero, unless the following relations are satisfied:

$$\omega_1 + \omega_2 = \omega_3 \tag{9}$$

$$\boldsymbol{q}_1 + \boldsymbol{q}_2 = \boldsymbol{q}_3 + \boldsymbol{g} \tag{10}$$

Equation (9) resembles the conservation law of energy since $\hbar\omega$ is a quantum of energy for a mode of frequency ω. It simply states the fact that two phonons with energies $\hbar\omega_1$ and $\hbar\omega_2$ combine to produce a third phonon with energy $\hbar\omega_3$ equal to the sum of the energies of the two phonons.

Although $\hbar\boldsymbol{q}$ represents crystal momentum rather than true inertial momentum, taking $\boldsymbol{g} = 0$ makes Eq. (10) look like the conservation law of momentum. Processes for which $\boldsymbol{g} = 0$ are called phonon–phonon N-processes (normal processes). By themselves, they cannot bring about a change in the direction of phonon flow—that is, they cannot dissipate heat and the thermal conductivity would be infinite. Although the N-processes make no direct contribution to the thermal resistance, they are nevertheless very important for the overall heat transport because they can, via their interaction with other phonons, redirect energy into other lattice modes that may relax faster than the original distribution. Processes for which $\boldsymbol{g} \neq 0$ are known as U-processes (umklapp processes). They are the cause of finite thermal conductivity because, following a collision, the direction of the flow of thermal energy is very different (substantially opposite) from the original direction, and this tends to relax the phonon distribution. The vector $\boldsymbol{g}$ is the reciprocal lattice vector. U-processes are dominant at high temperatures and it can be shown that they lead to the $1/T$-dependence of the thermal conductivity. As the temperature decreases, thermal conductivity increases, but even in the most perfect crystals the thermal conductivity does not grow without bounds at low temperatures because the mean-free path of phonons eventually becomes comparable with the physical dimensions of the crystal. When this happens, the phonon mean-free path attains a constant value, and the thermal conductivity is proportional to T^3, reflecting the behavior of the specific heat.

Superconductors are characterized by the pairing of electrons (Cooper pairs), which leads to the formation of a superconducting condensate at and below the superconducting transition temperature, T_c. The fundamental properties of superconductors—a complete loss of dc resistivity, and perfect diamagnetism (Meissner effect)—are reflections of the ability of the condensate to support a dissipationless supercurrent and to shield its interior from external magnetic fields. From the perspective of thermal conductivity, the superconducting condensate has three very important properties: (1) Cooper pairs carry no entropy and therefore the usual electronic thermal conductivity should vanish rapidly below T_c; (2) Cooper pairs do not scatter phonons, which means that the phonon mean-free path may increase as the sample is cooled below T_c; (3) electrons may be excited from the condensate into quasiparticle states (low-lying excitations of a superconductor), and this "normal gas" of particles, together with phonons, can carry heat below T_c. In principle, the quasiparticles can be used as probes of the superconducting condensate and they may help to shed light on the key issues such as the nature of the pairing state and its symmetry. Thermal magnetoresistance is an ideal tool for such investigations. To visualize the behavior of thermal conductivity, Fig. 2 shows sketches of typical trends in $\kappa(T)$ for (a) a dielectric crystal, (b) a good metal, (c) a conventional superconductor, and (d) a high-temperature superconductor.

MAGNETICALLY ORDERED STATES RELEVANT TO THERMAL MAGNETORESISTANCE

To assist the reader in understanding thermal magnetoresistance in materials in which magnetically ordered structure plays a pivotal role, here the most essential points concerning magnetism will be reviewed, and the concept of magnetic vortices (flux lines) in superconductors will be noted.

The magnetic moment of an atom originates from the orbital motion of an electron around the nucleus and its rotation around its own axis, called its spin. Both of these motions are quantized and can take up only certain discrete values and orientations in space. Orbital angular momentum, designated by the letter ℓ, can have any of the values $\ell = 0, 1, 2, \ldots, n - 1$, where n is the main quantum number. Electrons with angular momentum $\ell = 0, 1, 2, 3, \ldots$ are frequently referred to as the s, p, d, f, . . . electrons, the designation surviving from the heyday of atomic spectroscopy. The orientation of the orbital angular momentum with respect to an external magnetic field is specified by the magnetic quantum number, m_ℓ, which can have the values $m_\ell = -\ell, -\ell + 1, \ldots 0, \ldots \ell - 1, \ell$. The spin angular momentum of an electron in the direction of an external magnetic field has two components,

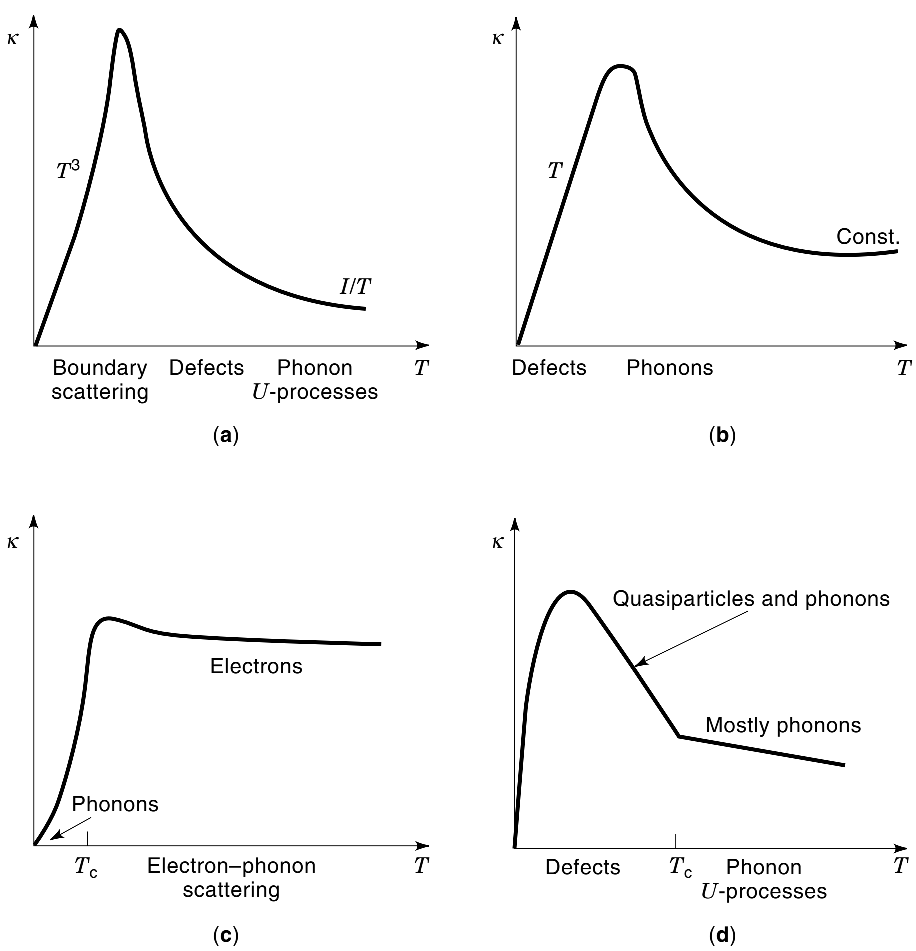

Figure 2. Sketches of typical behavior of thermal conductivity in (a) a dielectric crystal, (b) a good metal, (c) a conventional superconductor, and (d) a high-temperature superconductor.

$\pm\hbar/2$. It is usually stated that the spin of an electron has a quantum number $s = \pm 1/2$, understanding that this is in units of $\hbar$. The orbital angular momentum vector and the spin angular momentum vector add to form a vector of the total angular momentum specified by a quantum number $\boldsymbol{j}$, such that $\boldsymbol{j} = \boldsymbol{\ell} + \boldsymbol{s}$. For atoms with more than one electron, the contributions of all electrons have to be taken into account. When atoms are brought together to form a crystal, the orbital angular momentum of electrons is quenched (e.g., transition metals Fe, Co, and Ni) and each electron, through its spin angular momentum, contributes an elementary magnetic moment of one Bohr magneton ($\mu_B = 5.79 \times 10^{-5}$ eV T^{-1}).

Magnetic moment per unit volume, M, is called magnetization. Of great importance is the quantity called magnetic susceptibility, defined as $\chi = M/H$ where H is the magnetic field intensity. Materials with a negative susceptibility are called diamagnetic solids. They have closed atomic shells and their magnetic moment is induced in reaction to an external magnetic field. Materials with a positive susceptibility are paramagnets and they possess permanent magnetic dipoles. Two classes of magnetic materials, ferromagnetic and antiferromagnetic solids, also require the existence of permanent magnetic dipoles but, in addition, a strong interaction between the dipoles is essential. The dipoles must "cooperate" to form a spontaneous magnetic moment—that is, a nonzero magnetic moment even in the absence of an external magnetic field. The distinction between ferromagnetic and antiferromagnetic solids rests in the way the cooperative spins line up. In ferromagnetic solids all spins point in one direction, while in antiferromagnetic solids half of spins point in one direction, the other half in the opposite direction. Spontaneous magnetization associated with ferromagnetic solids persists from $T = 0$ up to some finite temperature T_C, called the Curie temperature. At the Curie temperature the ordered state of spins—that is, the spontaneous magnetization—vanishes, and for $T > T_C$ the material becomes a paramagnet. For antiferromagnetic solids, the effect is the same but Curie temperature (T_C) should be replaced by the Nèel temperature (T_N).

In the classical picture of magnetism, strong interactions that lead to a spontaneous magnetic moment are described in terms of the Weiss field. The modern quantum mechanical interpretation is based on the exchange field that arises as a consequence of the Pauli exclusion principle imposed on the electrons. Since no two electrons with the same spin can be at the same place at the same time (a restriction that does not apply to two electrons with opposite spins), the Pauli principle leads to two very different spatial configurations and, therefore, to two different electrostatic energy terms reflecting the parallel or antiparallel spin orientations. The difference in energy between the two spin configurations is the direct-exchange energy. Another important source of magnetic interaction is the so-called indirect exchange, by which the magnetic moments of pairs of ions couple through their interaction with conduction electrons.

For the transition metals of interest here (Fe, Co, and Ni), different tasks are assigned to different electrons, depending on the atomic orbitals from which they originally come. Electrons in the narrow but densely populated 3d-bands formed from the partially filled 3d-atomic orbitals are the "magnetic electrons" responsible for the magnetic properties of the transition metals. In contrast, the outer 4s-orbitals form broad 4s-energy bands. Electrons residing in the 4s-bands have a small effective mass and are thus highly mobile, and their primary assignment is to carry electric current. Although the 3d-electrons contribute only a small fraction of the total current, the high density of the 3d-band states in the vicinity of the Fermi level is very important for providing final states into which the 4s-electrons can be scattered as they interact with phonons, spin waves, impurities, and structural defects.

Do not forget that electrons can take up one of the two spin states—up or down. In 4s-bands, there are equal numbers of spin-up and spin-down electrons. This is not so in the 3d-bands. Because of the high densities-of-state in the 3d-bands, $D_d(E_F)$, and a rather large intra-atomic Coulomb repulsion, U (the interaction which favors parallel spins for the d-electrons and which gives rise to the spontaneous magnetic moments in the first place), the 3d transition metals satisfy the Stoner criterion:

$$(U/N)D_d(E_F) > 1 \tag{11}$$

Here N is the number of atoms in the crystal. Under the condition of Eq. (11), the 3d-band splits in such a way that the more populated spin-up band (majority spin band) shifts downward while the less populated spin-down band (minority spin band) shifts upward. A schematic representation of the spin-split 3d-bands for all three archetypal ferromagnets—Fe, Co, and Ni—is shown in Fig. 3. The majority and minority spin electrons are the essential ingredients to understanding the origin of the GMR effect described in the following section.

This section concludes with a few remarks concerning magnetic vortices. Superconducting condensate can be destroyed either by raising its temperature above the critical point, called the superconducting transition temperature, T_c, or by exposing the condensate to an external magnetic field larger than the thermodynamic critical field, H_c. The manner in which magnetic flux enters a superconductor when the field is strong enough leads to two distinct classes of superconductors: type I and type II materials. Since high-temperature perovskites are the extreme type II superconductors, this class only is considered.

An external magnetic field greater than the lower critical field—$H > H_{c1}$—drives a superconductor into a mixed-state in which single-quanta flux lines (vortices) penetrate the superconductor and form a regular 2-dimensional lattice. For

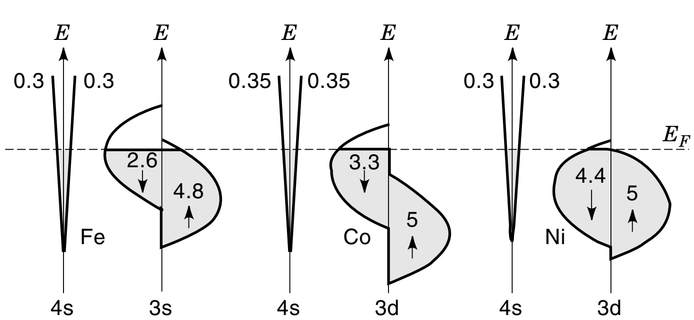

Figure 3. Schematic representation of the densities of state in the 4s and 3d bands of transition metals Fe, Co, and Ni. The numbers indicate electron occupancy of the spin-up and spin-down bands. The spin-split bands in these metals give rise to the majority and minority spin electrons that are the foundation of the GMR effect. Adapted from Mathon (4).

fields not much larger than H_{c1}, the vortices are widely separated but with increases in field intensity their separation decreases proportional to $H^{-1/2}$. The superconducting phase (condensate) is thus gradually squeezed out and, at $H = H_{c2}$ (upper critical field), the normal regions overlap and the superconducting condensate is destroyed. Vortices can be viewed as tubes of radius ξ (coherence length) containing bound excitations not too different from normal electrons. Around the core of the vortex circulates a supercurrent that shields the magnetic field of the vortex. Vortices are strong scatterers of phonons as well as of quasiparticles that may exist in the superconducting condensate. Because of the highly anisotropic crystal structure, vortices in the high-temperature perovskites may look not like rigid tubes, but rather like zigzag chains of soft pancakes. Nevertheless, their ability to impede thermal transport is undiminished and, in terms of their effect on the heat current at $T < T_c$, they leave fingerprints that provide a window into the world of unconventional superconducting materials. Thermal magnetoresistance in superconductors is intimately tied to the presence of magnetic vortices, and is the topic of the last section of this article.

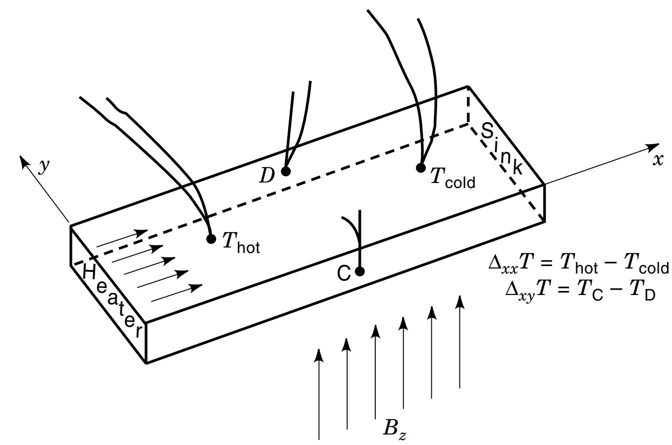

Figure 4. Generic experimental set-up for measuring thermal conductivity in a magnetic field. Thermocouple junctions A and B determine the longitudinal temperature difference $\Delta_{xx}T$, while the junctions at C and D measure the transverse temperature difference, $\Delta_{xy}T$. For measurements of GMR, the magnetic field is usually oriented along the direction of the heat.

EXPERIMENTAL TECHNIQUES OF THERMAL MAGNETORESISTANCE

To determine thermal magnetoresistance means to measure thermal conductivity in the presence of a magnetic field. Although heat flux, thermal gradient, and thermal conductivity have their natural analogs electric current, potential difference, and electrical conductivity, accurate thermal measurements are far more difficult to realize in practice than are their electrical counterparts. This is chiefly because in an electrical resistivity experiment current leakage paths can be virtually eliminated, while it is impossible to completely suppress all heat leakage paths in a thermal conductivity experiment. Great care must always be used to minimize heat leaks so that they can be considered negligible (or at least very small) with respect to the heat that passes through the sample. Materials considered in this review present a special challenge because of their structural form—often thin-films—and because of their small size—single crystals of high-temperature superconductors are not readily available in sizes exceeding a few millimeters.

In the temperature range where thermal magnetoresistance is of interest—usually at and below room temperature—the most convenient way to measure thermal conductivity is to use the longitudinal steady-state technique. This technique is the thermal analog of the four-probe bar measurement of electrical resistivity, and the generic experimental set-up is shown in Fig. 4. One end of the sample (crystal or thin film) is secured by mean of epoxy, solder, or by clamping to a temperature-controlled heat sink, which can be the cold tip of a low-temperature cryostat, the cold head of a closed-cycle refrigerator, or even a heated plate. An electric heater is attached in a similar manner to the free end of the sample. This heater may be a small wire-wound resistor, a strain gauge, or perhaps an evaporated metal film. For a given current I and voltage V across this electric heater, an amount of power $Q = I\ V$ will be produced. At two points, spatially separated by a distance L along the sample, are affixed temperature sensors that measure the temperatures T_{hot} and T_{cold} of the hot and cold side of the sample. Under the steady-state condition, and assuming all of the Joule heat generated by the heater flows down the sample, the temperature difference $\Delta T = T_{hot} - T_{cold}$ provides the measure of thermal conductivity via Eq. (2). Clearly, accurate determination of ΔT and the geometrical factor L/A are crucial to any meaningful measurement of thermal conductivity. The small size of samples dictates the use of thin thermocouple wires to determine ΔT. Differential thermocouple configuration is a distinct advantage, but one must not forget to insulate electrically at least one leg of the couple to prevent shorting of the couple through the sample.

Samples in the form of thin-films are normally deposited on some kind of a substrate, the thickness of which usually far exceeds the film's thickness. Since the substrate provides an excellent thermal short, one has no hope of determining the magnitude of the film's thermal conductivity correctly. This may not be a major problem, provided one is interested in changes in the thermal conductivity arising in the presence of a magnetic field rather than in the absolute value of the thermal conductivity. It nevertheless means that one must be able to resolve very small temperature changes, perhaps 0.1 mK or better, in order to detect the influence of a magnetic field. It is often advantageous to remove the film from the substrate or to deposit films on substrate that can be peeled off or dissolved.

The experimental set-up in Fig. 4 also serves well for measuring the Righi–Leduc effect, one of the transverse thermomagnetic coefficients that happens to be a thermal equivalent of the Hall effect. In this case, in addition to measuring the longitudinal gradient $\nabla_x T$, one also needs to measure the transverse thermal gradient $\nabla_y T$, which is accomplished by a second differential thermocouple connected at points C and D in Fig. 4. This arrangement is the basis of thermal magnetoresistance measurements discussed in the last section of this article. More details and other techniques to measure thermal conductivity are discussed in Berman (5) and Uher (6).

THERMAL MAGNETORESISTANCE IN GMR STRUCTURES

Spectacular development in the technology of thin-film deposition, including techniques such as molecular beam epitaxy (MBE), chemical vapor deposition (CVD), and laser-assisted sputter deposition (LASP), among others, has facilitated the growth of novel thin-film structures with unique physical properties. In the hands of skilled material scientists and engineers, these techniques represent an unprecedented opportunity to grow and control materials one atomic layer at a time and create exotic structures that nature is incapable of creating. These developments have allowed scientists to peek into the properties of lower-dimensional (mostly 2-dimensional) solids, and on numerous occasions they have had a direct impact on the design and production of state-of-the-art electronic devices and sensors.

Among the most fascinating novel material configurations that owe their existence to recent advancements in deposition techniques are artificially created multilayers and superlattices containing layers of magnetic material. Although there has always been an interest in the magnetic properties of thin films, the discovery in the late 1980s of an unusually large magnetoresistance called giant magnetoresistance (GMR) and, concurrent with it, an oscillating magnetic coupling, have energized the interest of the scientific community. The elegance of the physical concept that underscores the GMR effect, together with the promise this phenomenon holds for exciting device applications, has ignited vigorous research activity worldwide (7).

Giant magnetoresistance refers to large changes in the resistance of magnetic nanoscale structures (multilayer films and granular magnetic structures) brought about by an external magnetic field as it forces a change in the orientation of the magnetic moments in the layer strata. There are several different configurations of magnetic structures that have been shown to exhibit large magnetoresistance effects. They include the following: (1) multilayer films made with alternating ferromagnetic layers of different coercivities that have very low "switching" fields and hold promise for magnetorecording devices; (2) spin-valve sandwiches, which consist of two ferromagnetic layers separated by a nonmagnetic spacer layer. The magnetization direction of one of the ferromagnetic layers is pinned and that of the other is free to rotate so that its magnetization can be rotated with the aid of an external magnetic field from the parallel to the antiparallel alignment; (3) exchange-coupled magnetic structures; and (4) granular magnetic structures. Although the physical mechanisms that underpin the low- and high-resistance states differ in details, the essential ingredient of all of them is the asymmetry in spin-dependent scattering of conduction electrons. This concept will be illustrated with the last two categories of magnetic structures—exchange-coupled multilayers and granular films. These are the structures on which most of the thermal magnetoresistance studies have been conducted.

Figure 5(a) depicts an exchange-coupled multilayer structure. The term exchange-coupled means that two magnetic layers that are physically separated can "communicate" with each other via an indirect exchange interaction with conduction electrons in a nonmagnetic spacer layer. In exchange coupled GMR structures, under zero field conditions, the two magnetic layers are lined up so they are magnetized in opposite directions—that is, they are ordered antiferromagnetically. Because of the oscillating nature of coupling, one can always adjust the separation (by varying the thickness of the nonmagnetic spacer layer) at which the two magnetic layers couple antiferromagnetically.

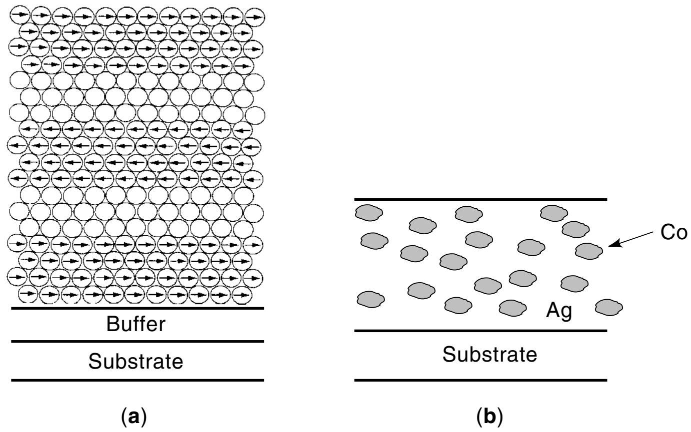

Figure 5. Schematic layout of (a) an exchange-coupled magnetic multilayer showing ferromagnetic layers coupled across noble metal spacer layers in an antiferromagnetic alignment, and (b) granular magnetic structure with randomly distributed grains of cobalt in a silver matrix. Sizes of cobalt grains depend on the preparation and annealing treatments but are typically on the order of several nanometers.

Exchange-coupling across a nonmagnetic spacer layer was first seen in rare-earth-based multilayers consisting of gadolinium and yttrium. In this case, the localized magnetic moments of the rare earth that are responsible for the long-range oscillatory exchange-coupling can be explained quite naturally by the Rudermann–Kittel–Kasuya–Yosida interaction, the well-known RKKY model. The magnetic layers in the GMR structures of interest are virtually always fabricated from the 3d transition metals (Ni, Fe, Co) and their alloys. Although the magnetic moments in these transition metal ferromagnets have a substantially itinerant character, oscillations in the exchange coupling have been well documented for a large number of 3d transition metal ferromagnets with a variety of noble- or transition-metal spacer layers. Indeed, it is more a rule than an exception to observe coupling oscillations in such systems.

Typical layer separation (oscillation period) over which the coupling switches from a ferromagnetic to an antiferromagnetic alignment, or vice versa, is on the order of 1 nm, although more than one period may be present in some systems. The coupling strength can be obtained from the hysteresis loops, and it falls in the range 10^{-3} J/m^2 to 10^{-2} J/m^2 or, equivalently, 1 erg/cm^2 to 10 erg/cm^2.

The antiferromagnetic alignment of the magnetic layers represents a high-resistivity state. With the aid of an external magnetic field, one aims to break the exchange coupling and rotate the magnetic moments of the layers so that all are aligned ferromagnetically. This configuration represents a low-resistivity state. The difference between the high- and low-resistivity states or, more precisely, the percentage of this difference, is the measure of the magnitude of the magnetoresistance. For the best of structures, usually Fe/Cr and Co/Cu multilayers, the changes in the resistance are very high and may exceed 65% at room temperature. Such large magnetoresistance corresponds to a complete rotation and saturation of the magnetization and typically requires magnetic fields in excess of 1000 Oe. Fields of this magnitude are too high for many practical applications.

Figure 5(b) shows a very different magnetic structure. Instead of well-defined magnetic layers, one has randomly distributed nanoscale magnetic granules (Co, Fe, Ni) dispersed in a nonmagnetic metal matrix (usually Cu or Ag). Such structures are prepared either by sputtering followed by annealing or by coevaporation in an MBE chamber at modest growth temperatures, which leads to spontaneous phase separation of the constituents. Since there is no exchange coupling between the grains, the magnetic moments are randomly oriented in a zero external field, which corresponds to a state of high resistance. Applying an external magnetic field causes the grains to rotate their moments in the direction of the field. When all grains are magnetized parallel to one another, the resistance reaches its minimum. Magnetoresistances in excess of 70% at 4.2 K and near 25% at room temperature are possible. Although the saturation fields are rather high, attempts are being made to reduce it by shaping the granules to make it easier to rotate the magnetic moments.

As already noted, giant magnetoresistance arises as a consequence of the asymmetry in the spin-dependent scattering of conduction electrons. To illustrate the point, consider an exchange-coupled multilayer with magnetic layers made of 3d transition metals (Fe, Co, Ni, and their alloys). The 3d band is spin-split, giving rise to majority and minority spin bands. Because the spin relaxation time in ferromagnetic transition metals significantly exceeds the momentum relaxation time, it takes several momentum-randomizing collisions before the electron flips its spin. In other words, the electron keeps memory of its spin orientation for a comparatively long time. This allows one to view the conduction electrons as forming two distinct parallel channels, one for spin-up electrons and one for spin-down electrons—the essence of the two-current model of Campbell and Fert (8).

Assume that the magnetic layers under zero field conditions are aligned antiferromagnetically as in Fig. 6(a), and

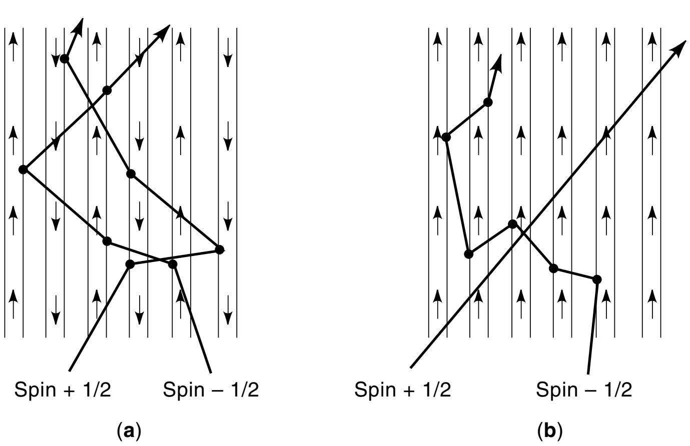

Figure 6. Schematic view of the spin-up and spin-down trajectories in an exchange-coupled magnetic multilayer in (a) a zero magnetic field, where the layers are aligned antiferromagnetically; and (b) an external magnetic field strong enough to line up the magnetization of all layers. The mean-free path of electrons within the layers is assumed to be much larger than the individual layer thickness so that electrons "sample" several magnetic layers.

the current is applied parallel to the interfaces, the so-called CPI configuration. If, after the current is injected into the structure, the paths of the conduction electrons were to remain strictly along the layer strata (channeling effect), there would be no magnetoresistance effect, as most of the current would be shunted by the high-conductivity nonmagnetic spacer layers. It is because of electron scattering that the conduction electrons quickly acquire a component of momentum perpendicular to the layers, cross the interfaces, and enter the magnetic layers.

Why not apply the current perpendicular to the planes (CPP configuration) in the first place? While such studies have been done, there are considerable experimental obstacles to assuring meaningful measurements under CPP conditions. Quite apart from the challenge of making electric contacts between the substrate and the first deposited layer—that is, "underneath" the structure—one also faces an unfavorably small geometrical factor, L/A, that relates the resistance to the resistivity ($R = \rho L/A$), and thus the voltage signal across the multilayer is very small. Lithography must usually be employed to make the geometrical factor more reasonable so that the signal can easily be resolved. Because of this complication, the vast majority of experimental studies are carried out with the current applied parallel to the interfaces—that is, in the CPI geometry.

Because of their long spin relaxation time, as the spin-up (majority) and spin-down (minority) conduction electrons cross into the magnetic layers or are scattered at the interfaces, they both encounter roughly the same number of low- and high-resistance regions (remember, it is assumed that the successive magnetic layers are coupled antiferromagnetically). The majority and minority electrons find it easier to traverse the regions where the magnetization is parallel to their respective spin orientations, while in the regions where the magnetization is opposite to the electron spin the resistance is high and electron motion tends to be impeded. Since each spin channel is affected roughly equally and each has an averaged resistivity of $(\rho\uparrow + \rho\downarrow)/2$, where $\rho\uparrow$ and $\rho\downarrow$ are the resistivities of the spin-up and spin-down electrons, respectively, the total resistivity corresponding to the initial antiferromagnetic alignment of the magnetic layers in a zero external magnetic field is

$$\rho_{\mathrm{AF}} = \frac{\rho\uparrow + \rho\downarrow}{4} \tag{12}$$

With an external magnetic field of sufficient strength to overcome the antiferromagnetic coupling, the magnetization rotates from an antiparallel to a parallel alignment, [Fig. 6(b)]. Now the electrons encounter a very different environment. The spin-up electrons experience smaller resistance as they move in the structure because their spins are favorably aligned with the magnetization. In contrast, the spin-down electrons tend to be strongly scattered at the interfaces and in the bulk of the magnetic layers because they encounter an "unfriendly" orientation of magnetization. Since the two spin channels are independent and thus conduct in parallel, the resistivity of the structure in the magnetic field that produced the ferromagnetic alignment of the magnetic layers is

$$\rho_{\mathrm{F}} = \frac{\rho\uparrow\rho\downarrow}{\rho\uparrow + \rho\downarrow} \tag{13}$$

Because the spin-up electrons provide a low resistance path they effectively shunt the current and the total resistivity is low. The magnetoresistance of the structure is defined in terms of ρ_{AF} and ρ_F and, after a straightforward manipulation of Eqs. (12) and (13), is given by

$$R \equiv \frac{\rho_{AF} - \rho_F}{\rho_{AF}} = \left(\frac{\rho\downarrow - \rho\uparrow}{\rho\downarrow + \rho\uparrow}\right)^2 = \left(\frac{\alpha - 1}{\alpha + 1}\right)^2 \tag{14}$$

Here $\alpha = \rho\downarrow/\rho\uparrow$ is the asymmetry parameter. In deriving Eq. (14) one tacitly assumes that the conduction electrons traverse many layers—that is, that the electron mean-free path is much larger than the layer thickness. This is not an unreasonable assumption since the thickness of layers in these structures is typically a few nanometers and the mean-free path along the layers is on the order of 10 nm or more. In any case, as long as the electrons can "sample" more than one magnetic layer the magnetoresistance will exist. The other issue neglected while deriving Eq. (14) concerns mixing of the spin channels due to the electrons being scattered by magnons (quanta of spin-wave excitations). Magnon scattering obviously has a detrimental influence on the magnetoresistance because it compromises the purity of the spin channels and it causes the conduction electrons to lose the memory of their spin state more quickly. The influence of spin-mixing is reflected in the lower values of magnetoresistance at ambient temperatures (by a factor of 2–3, depending on the structure), in comparison to the values measured at the liquid helium temperature.

A question of paramount importance is where exactly spin-dependent scattering comes from. Does it originate in the interior of the magnetic layers as in the bulk transition metal ferromagnets, where the d-bands have high densities of state (DOS) at the Fermi level and s-d scattering dominates the transport? Or are the interfaces between the magnetic and spacer layers the source of asymmetry in spin scattering? If the latter is the case, is it just potential scattering at interfaces that matters, or does the asymmetry in the DOS of the spin-up and spin-down d-bands play a role? While the results of careful experiments in which minute amounts of magnetic material were introduced near the interface (planar doping) seem to indicate that interfaces play the dominant role, the question of the role of scattering potential versus the role of DOS cannot be answered by experiments limited to studies of magnetoresistance, because both viewpoints predict the same behavior. Other investigations are called upon to shed light on the underlying physics and thermal transport measurements are among the most effective methods in this regard. For example, investigations of the thermoelectric power in a magnetic field revealed a correlation between the magneto-thermopower and the magnetoresistance of the form $S(H, T) \propto 1/\rho(H, T)$ for numerous multilayer and granular systems. This implies a strong field dependence of the thermopower which, in turn, suggests that the DOS of the ferromagnetic layers and granules play the dominant role in spin-dependent scattering.

There is interest in the behavior of thermal magnetoresistance and in what additional input it provides into the issues concerning the mechanism of GMR. As discussed earlier, the Wiedemann–Franz law is a powerful tool to determine whether the carrier scattering is elastic or whether the interaction includes a change in the carrier's energy. Clearly, any proof of inelasticity in the conduction electron scattering guides the choice of an appropriate model of transport.

To assess the validity of the Wiedemann–Franz law directly, one needs first to determine the magnitude of the electronic thermal conductivity. In thin films and multilayers (the usual structural forms of GMR devices) the measurement of thermal conductivity is complicated by several factors. First of all, the films are deposited on some kind of a substrate (glass, silicon, GaAs, etc.) that typically has a far larger thermal conductance than the deposited film itself. The substrate thus provides a thermal shunt, and an accurate determination of the film's thermal conductivity is not possible. Furthermore, the thermal conductivity of a multilayer consists not only of the electronic component—there are also contributions due to phonons, and even magnons may participate in the heat transport. Magnons are quanta of spin waves that can be excited in a magnetic system, and they may be viewed as a train of flipping spins propagating in the system. There is an energy content—that is, heat—associated with propagating magnons. Moreover, under certain conditions, magnons may scatter electrons and alter their distribution function. Clearly, it is a complex problem and it is unlikely that one would be able to ascertain the individual thermal conductivity contributions with great accuracy merely by measuring the thermal conductivity of a multilayer in a zero magnetic field. It is here where thermal magnetoresistance comes into play as an important transport parameter.

Since the substrate is usually an insulator, the magnetic field will have no effect on its thermal conductivity. Likewise, the phonon thermal conductivity is insensitive to the external magnetic field. This leaves just the electrons, and from the preceding discussion it is known that the electric current is strongly influenced by the magnetic state of the structure. It is thus no surprise that the thermal energy—that is, the heat—associated with the flow of the electrons should also be strongly influenced by the magnetization of the film. All one has to do is to ensure that the thermal conductance of the film or multilayer is not too small a fraction of the total thermal conductance so that one has a chance to resolve the change in the thermal conductivity upon application of an external magnetic field.

There are two obvious approaches to maximizing the resolution: either to deposit a multilayer with a very large number of layers, or to make sure that the conductance of the substrate is as small as possible. Although one has some control over the thickness of the deposited structure, it is difficult and exceedingly time consuming to deposit high-quality multilayers with a thickness greater than 1 μm using an MBE system, and even sputtering techniques are challenged by these very thick film strata. It is often more advantageous to diminish the influence of the substrate by either: (1) depositing the multilayer on a thin insulating substrate film (e.g., Kapton), (2) fabricating as thick a multilayer as practicable and then removing it from the backing material, or (3) depositing the structure on specially developed "removable substrates," such as synthetic fluorine mica that can be peeled off from the multilayer. It should be stated that even without these special precautions one can detect thermal magnetoresistance in GMR structures provided the temperature difference along the sample is monitored continuously and with a resolution of 1 mK or better. A generic experimental set-up is shown in Fig. 4, and a magnetic field is applied parallel to the layers—that is, along the direction of heat flow.

At a given temperature and for a constant heater power, the variation in ΔT as the magnetic field is swept corresponds directly to the changes in the thermal conductivity (or its inverse, thermal resistivity) of the magnetic multilayer. These changes can be large and, in analogy to giant magnetoresistance, they are referred to as giant magnetothermal resistance (GMTR), with its inverse called giant magnetothermal conductivity (GMTC). Monitoring variations in the electrical and thermal transport as a function of the magnetic field in the same samples (either granular or multilayer structures), one can relate GMTR (or GMTC) with GMR. From the relation between GMTC and GMR one can make conclusions about the validity of the Wiedemann–Franz law and the nature of carrier scattering. As an example, Fig. 7 shows the field dependence of thermal conductivity plotted as $\partial\kappa = \kappa(H) - \kappa(0)$ (GMTC value here is 28%), and electrical conductivity ($\sigma = 1/\rho$) plotted as $\partial\sigma = \sigma(H) - \sigma(0)$ at a temperature of 72 K for a thick-film of the granular magnetic structure $Co_{20}Ag_{80}$. Similar plots apply throughout the temperature range 4 K to 300 K. It is obvious that both $\partial\kappa$ and $\partial\sigma$ have the same field dependence. Thus, at a given temperature, the relative variations in both quantities are the same, attesting to the validity of the Wiedemann–Franz law and confirming the common physical origin of the effects. In turn, this implies that the carrier scattering at the interfaces and within the Co granules and the Ag matrix is essentially elastic and certainly of large angle. Any kind of inelastic scattering, even in the temperature regime above 100 K where it usually dominates, must be incoherent—that is, not conserving the wave vector $\boldsymbol{q}$.

Thermal magnetoresistance of magnetic multilayers has been studied more widely and the results seem to concur with those obtained on granular magnetic systems. To illustrate the general validity of the Wiedemann–Franz law and the ensuing elasticity of carrier scattering in GMR structures,

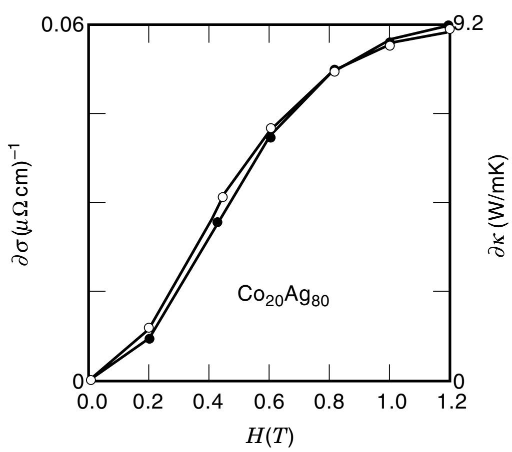

Figure 7. Changes in the electrical conductivity, $\partial\sigma = \sigma(H) - \sigma(0)$, and thermal conductivity, $\partial\kappa = \kappa(H) - \kappa(0)$, as a function of magnetic field for the granular magnetic structure $Co_{20}Ag_{80}$. The essential point is the same field dependence of both $\partial\sigma$ and $\partial\kappa$, implying that the charge carriers scatter elastically. Data are from Piraux et al. (9).

Fig. 8 shows data obtained on a magnetic multilayer (superlattice) made by alternating layers of cobalt and copper in a molecular beam epitaxy (MBE) system. This single crystalline structure, with its atomically smooth interfaces and its perfect layering sequence, is—in terms of its structural perfection—the antithesis of the randomly distributed granular magnetic structure. The multilayer consists of 215 bilayers of (111)-oriented Co and Cu (7 monolayers of cobalt alternating with 19 monolayers of copper for a total thickness of slightly over 1 μm) deposited on a substrate of synthetic fluorine mica with a Rh(111) buffer to initiate the (111)-oriented layer growth. The mica was subsequently cleaved off the metal film, leaving a “freestanding” film. Both electrical resistivity and thermal conductivity exhibit more than 10% change as the field increases to saturation, and they correlate with each other. It is interesting to note that the saturation field for the magnetotransport is much larger than the saturation field for the measured magnetization. The lack of correlation with the magnetization of the Co layers confirms that spin-dependent scattering of conduction electrons occurs not in the interior of the Co layers but evidently near the Co/Cu interfaces. Figures 8(a) and 8(b) show scaling between the GMTC and GMR for the same magnetic multilayer at 80 K and 150 K. Linear dependence observed between $\kappa(H)$ and $T/\rho(H)$ over a wide range of temperatures validates the Wiedemann–Franz law, and suggests the common scaling for different temperatures.

THERMAL MAGNETORESISTANCE IN COLOSSAL MAGNETORESISTANCE STRUCTURES

While the giant magnetoresistance effect in heterogeneous materials such as magnetic multilayers and granular magnetic films is an exciting phenomenon with considerable technological potential, large negative magnetoresistance is not limited to GMR structures only. There are numerous reports in the literature of a magnetic field causing a dramatic change in a sample’s resistance. In terms of the sheer magnitude of the resistivity change, perhaps the most spectacular example (11) is a heavily doped antiferromagnetic semiconductor—EuSe. In the liquid helium temperature range and in a magnetic field set to zero, EuSe with a carrier density of less than 10^{19} cm^{-3} has very high resistivity, on the order of 10^7 Ω cm. On application of an external field of no more than 1 T, the resistivity drops down to the 10^{-2} Ω cm range. As impressive as the nine orders of magnitude change is, it is of little practical use because this field-driven antiferromagnetic-ferromagnetic transition is limited to very low temperatures.

Far more promising are the magnetoresistance effects in manganese oxide-based perovskites. Benefiting from an intensive worldwide search for novel high-temperature superconductors in the cuprate perovskites, and further boosted by the exciting discovery of the GMR effect, the last five years or so have witnessed a major revival in the study of manganite perovskites. Although the fundamental physical properties of this material have been known for nearly fifty years, advances in thin-film deposition enabled fabrication of high-quality films with well-controlled doping levels, which ultimately led to the observation of negative magnetoresistance that far exceeds the values achieved with GMR structures. The magnitude of the magnetoresistance effect in manganite

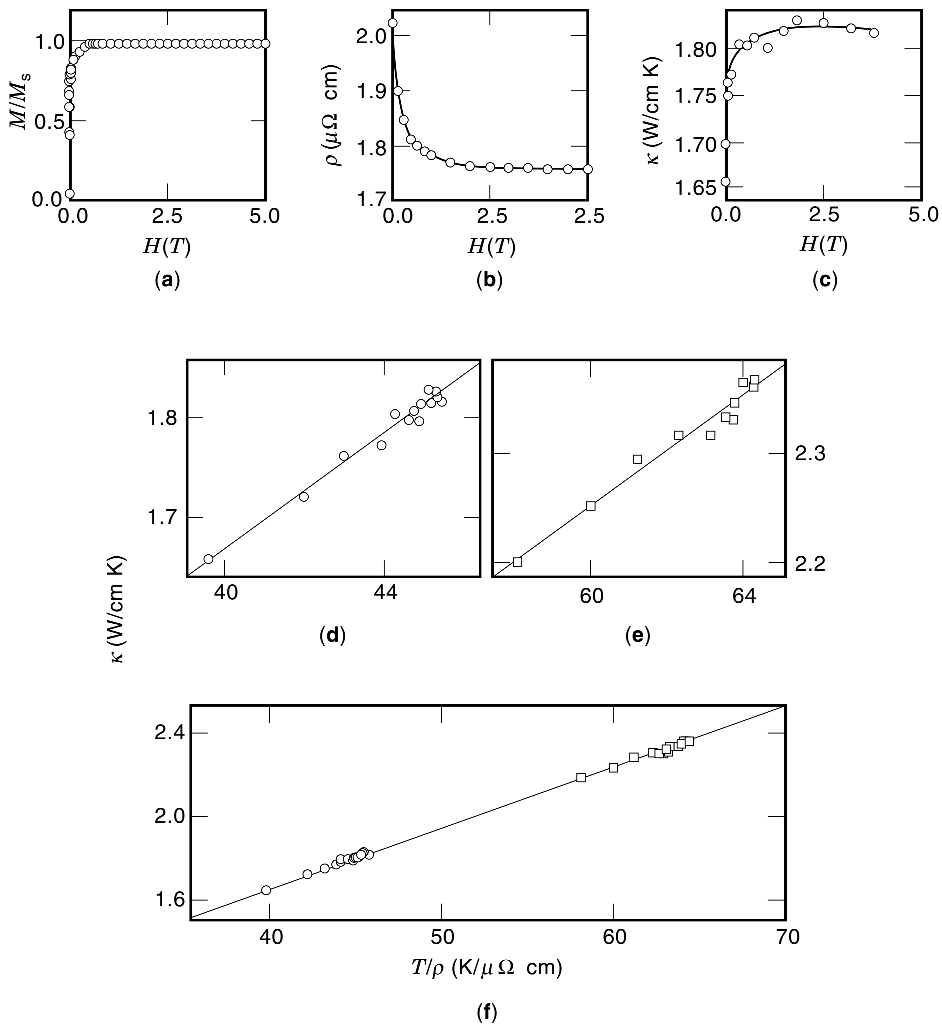

Figure 8. Field-dependent properties of a Co/Cu multilayer at 80 K. The upper three panels indicate the behaviors of (a) magnetization, (b) resistivity, and (c) thermal conductivity. The lower panels show scaling plots of magnetothermal conductivity, $\kappa(H)$, and magnetoresistance, $\rho(H)$ at (d) 80 K, and at (e) 150 K. A temperature-dependent scaling plot of $\kappa(H, T)$ versus $T/\rho(H, T)$ at 80 K (circles) and 150 K (squares) is shown in panel (f). The lines through the points are linear fits of the data with slopes that correspond to a Lorenz number of $(2.7 \pm 0.3) \times 10^{-8}\ V^2/K^2$. Data are from Tsui et al. (10).

perovskites proved spectacular, and a new term was coined to describe it—colossal magnetoresistance (CMR). As the discovery of this effect is an important development and thermal magnetoresistance measurements have been made on this magnetic system, one should review the essential physics underpinning this effect.

The parent structure is an antiferromagnetic insulator, $LaMnO_3$, with the Nèel temperature of about 140 K. With a trivalent La^{3+} ion and three O^{2-} ions, charge neutrality dictates that the manganese be in the Mn^{3+} state. This implies the presence of four d-electrons; in standard notation, the electronic configuration of Mn^{3+} is $3d^4$. The octahedral crystal field splits the five-fold orbital degeneracy of the d-level into threefold degenerate t_{2g} orbitals and higher lying (by a few eV) twofold degenerate e_g orbitals. Three of the four Mn^{3+} electrons occupy the tightly bound t_{2g} orbitals. These orbitals remain highly localized and, because of a strong intraatomic Hund's coupling that tends to maximize the local magnetic moment consistent with the Pauli exclusion principle, all three t_{2g} electrons line up with the maximum spin of 3/2. The material's electronic activity is associated solely with the single remaining and substantially itinerant electron that occupies the e_g state. Again, due to the strong Hund's coupling, the spin of this electron lines up parallel with the core electrons. Furthermore, strong on-site Coulomb repulsion assures that no d-orbitals are occupied by more than one electron. This all conspires to make $LaMnO_3$ a Mott-type antiferromagnetic insulator.

A very different picture emerges upon a partial substitution of the La^{3+} ion with a divalent A^{2+} ion of alkaline earth and the formation of the mixed-valence manganite perovskite family $La_{1-x}A_xMnO_3$, where A = Ca, Sr, or Ba. For $0 < x < 0.2$ and for $x > 0.5$, the ground state of the system is either antiferromagnetic or possibly ferrimagnetic (for small x values) and is, in either case, electrically insulating. As such, these ranges of concentrations are of no direct interest to the description of the CMR effect. In contrast, of considerable interest is the range of concentrations $0.2 < x < 0.5$. Here the originally insulating $LaMnO_3$ is driven into a metallic state (i.e., the temperature coefficient of resistivity is positive even though the magnitude of the resistivity is more akin to those of degenerate semiconductors than of good metals) and, simultaneously, the antiferromagnetic spin order evolves into a ferromagnetic state. In this concentration range, an external magnetic field will assist in aligning the spins ferromagnetically with an accompanying low-resistivity state and will give rise to the phenomenon of colossal magnetoresistance. It follows that for $0.2 < x < 0.5$, there exists a Curie temperature, T_C, (typically somewhere between 150 K and 350 K) below which $La_{1-x}A_xMnO_3$ is a fully polarized ferromagnetic metal and above which it is a paramagnetic solid with electrical resistivity that may have an activated character. As the sample is cooled through T_C, the resistivity drops sharply and becomes strongly field sensitive. The highest values of colossal magnetoresistance are usually associated with lower T_C systems.

How exactly the magnetic order and the conduction process are tied together and how they evolve and change at T_C is a subject of much debate, and a complete theoretical description is still being refined. The usual starting point is Zener's idea of "double exchange (12)," which relies on the existence of a mixed valence state of manganese and assumes a strong Hund's coupling in the system. It works something like this: In $La_{1-x}A_xMnO_3$, the fraction $(1 - x)$ corresponds to the Mn^{3+} state, while overall charge neutrality necessitates that the x fraction (amount of the divalent rare earth) corresponds to the Mn^{4+} state. The latter ion has one less electron and compensates for the charge-deficient A^{2+} ion. Manganese thus appears in two distinct electronic configurations (i.e., it has a mixed valence)—the Mn^{3+} state with three electrons in the t_{2g} orbitals and a single electron at the e_g level, and the Mn^{4+} state which has no electrons in the e_g orbital (see Fig. 9). As already noted, strong Hund's coupling aligns spins of all d-electrons of a given ion. Assuming that both Mn^{3+} and Mn^{4+} ions are in the neighborhood, the essence of the double exchange rests in the notion that when an e_g electron tries to hop from the Mn^{3+} ion to an empty e_g level of the Mn^{4+} ion, it can do so effectively only when the core electron spins (those in the t_{2g} levels) of the two ions line up in parallel. Hopping—that is, charge transport—between manganese ions with core spins in the antiferromagnetic configuration is very inefficient. The double exchange mechanism thus clearly links charge transport with magnetic order.

As elegant as the double exchange appears to be, it unfortunately underestimates the magnitude of the CMR effect, and the scattering resulting from spin disorder is simply of insufficient strength to account for large resistivities observed in the insulating state above T_C. The double exchange thus does not capture the entire physical reality pertinent to the problem. Indeed, strong evidence exists that other interactions may be at play, particularly in the lower T_C systems. For instance, a strong Jahn–Teller based electron–phonon coupling might lead to localization of the conduction electrons as polarons above T_C. The Jahn–Teller distortions are combinations of the lattice modes that change either the Mn–O bond length or the bond angle and thus have a profound effect on the coupling (overlap integral) between the Mn ions. There are various scenarios for how the oxygen octahedral environment around a Mn site gets distorted and how the distortions couple to the charge fluctuations on the Mn site. These scenarios are beyond the scope of this article. Here it should suffice to note that the full physical picture is exceedingly complex and involves the coupling of the structural, magnetic, and transport properties which, in turn, are governed by the interplay among the lattice, spin, and charge degrees of freedom.

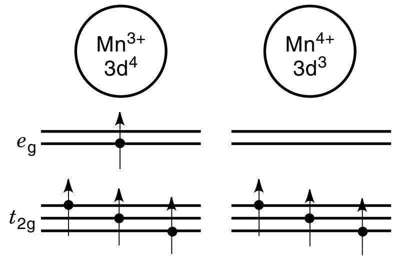

Figure 9. Electronic configuration of the Mn^{3+} and Mn^{4+} ions that is essential for the double-exchange model of the colossal magnetoresistance effect.

Heat transport in CMR materials is characterized by a surprisingly low thermal conductivity value. Regardless of whether one measures sintered samples or single crystals, the magnitude of the thermal conductivity of manganite perovskites is only a few $Wm^{-1}K^{-1}$, a value that is more representative of amorphous solids than of crystalline materials. Furthermore, an estimate of the electronic thermal conductivity of CMR materials based on electrical resistivity data and the Wiedemann–Franz law suggests that phonons (lattice vibrations) are by far the dominant heat-conducting entities. At temperatures near and above the Curie temperature, the electronic thermal conductivity is no larger than a couple of percent of the total thermal conductivity, and only at very low temperatures, $T \ll T_C$, may the conduction electrons play any significant role in heat transport. Because of the very low thermal conductivity, heat carried by magnons (spin waves) may represent a higher percentage of the total heat flow than is typical in magnetic insulators. Nevertheless, estimates based on the size of the magnetic specific heat anomaly at the Curie temperature indicate that the magnon contribution is unlikely to exceed 5% to 10% of total heat conduction even near T_C. Thus for all practical purposes, heat in the manganite perovskites is carried by phonons. The questions are why is it so inefficient, and what causes the phonon mean-free path to be no larger than the lattice spacing, as the magnitude of the thermal conductivity implies? These are pertinent questions, especially when one takes into account that the closely related cuprate perovskites—superconducting as well as insulating—exhibit thermal conductivities that are an order of magnitude larger.

With the conduction electrons "tied" in some kind of polaronic formation at $T \geq T_C$ (small polarons and magnetic polarons are the frequently invoked scenarios), the most likely strong phonon scatterers are spin fluctuations near T_C and static local distortions of the octahedral environment surrounding each Mn ion that are effective at and above T_C. As both spin fluctuations and local distortions weaken rapidly when the material transforms into the ferromagnetic state, the thermal conductivity is expected to increase.

Thermal magnetoresistance offers strong supporting evidence for this viewpoint. Because an external magnetic field tends to line up the spins and thus suppress spin fluctuations as well as static distortions, one expects the thermal conductivity to increase in the presence of a magnetic field. As shown in Fig. 10, this is exactly what happens (13). The enhancement of the thermal conductivity in a magnetic field is truly spectacular, amounting to up to 30% near T_C. Values of this magnitude provide irrefutable evidence for strong phonon scattering on both the structural and spin disorder in the manganite perovskites. Thanks to thermal magnetoresistance one has a technique that assesses the role of phonon dynamics and the important interactions phonons undergo via their coupling to local structural distortions and the spin degrees

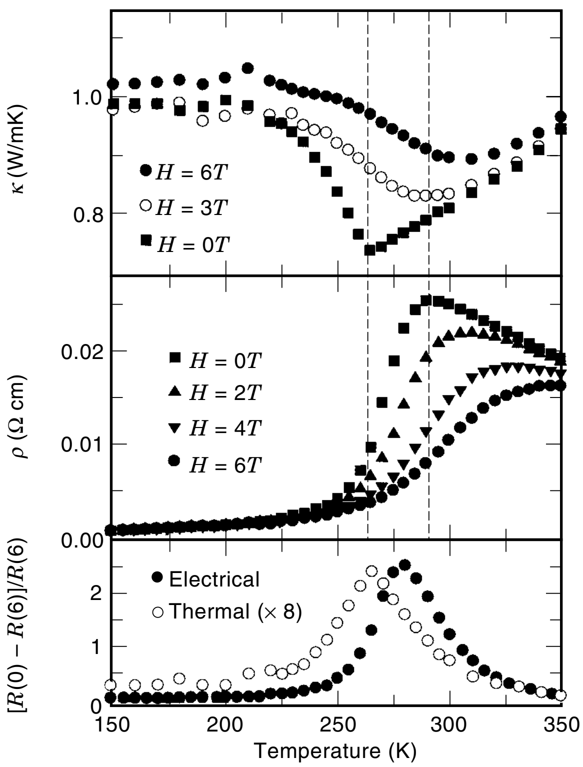

Figure 10. Field dependence of thermal conductivity (upper panel), electrical resistivity (middle panel), and the respective magnetoresistances as a function of temperature for crystal of $La_{0.2}Nd_{0.4}Pb_{0.4}MnO_3$. The peaks in the magnetoresistance and thermal magnetoresistance do not coincide but differ by about 15 K in this case. In other investigations the peaks are reported to coincide. Data are from Visser et al. (13).

of freedom, information that is not available from usual CMR measurements.

THERMAL MAGNETORESISTANCE IN HIGH-TEMPERATURE SUPERCONDUCTORS

A characteristic feature of heat transport in the high-temperature perovskites is a sudden rise in the thermal conductivity below T_c, which leads to a spectacular peak in $\kappa(T)$ at temperatures near $T_c/2$, (see Fig. 2(d)). Whether this effect is due to phonons or to quasiparticles has been the subject of much controversy. Initial interpretation viewed the rise in $\kappa(T)$ as due to phonons—their mean-free path increasing because phonon–electron scattering weakens as the electrons (or holes) condense into a superconducting condensate. As more was learned about the properties of high-temperature superconductors, it became obvious that the condensate has very unusual characteristics, among them the ability to sustain residual normal (i.e., nonsuperconducting) fluid to very low temperatures, and quasiparticles (low-level excitations) with an exceptionally long relaxation time. These findings led to a reinterpretation of the low-temperature thermal conductivity peak in terms of an electronic origin. Since both viewpoints—phonons and quasiparticles—provide excellent fits to the experimental data, the aim was to find an experimental probe which would decide the issue. It was hoped that the use of a magnetic field might offer a new angle on the role of carriers and phonons in thermal transport. While thermal magnetoresistance results show a strong influence of a magnetic field on thermal conductivity (up to a 30% decrease in a field of 5 T), the interpretation of the longitudinal thermal conductivity data in an external magnetic field remains equivocal—both phonons and quasiparticles may scatter on vortices, and both interactions would lead to similar degradation of thermal conductivity in an increasing magnetic field (14).

Even though these experiments could not address the origin of the peak in $\kappa(T)$ below T_c, this effort stimulated new approaches to exploring nontraditional thermal transport probes rather than just those appropriate for probing longitudinal thermal magnetoresistance. These approaches proved fruitful; new results not only provide a firm estimate of the relative importance of phonons and quasiparticles, but also offer exciting prospects for investigating fundamental issues concerning the nature of high-temperature superconductivity, such as quasiparticle dynamics and the symmetry of the pairing state. It should be remembered that the superconducting condensate is an extremely efficient electric shunt, and it is thus difficult or even impossible to investigate many low-temperature phenomena by electrical means; hence the importance of thermal magnetoresistance effects, which circumvent this problem.

The experiments make use of one of the less well-known transport phenomena—the Righi–Leduc effect. In essence, this effect is a thermal equivalent of the Hall effect and here it shall be called the thermal Hall effect. The idea here is to take advantage of the transverse thermal conductivity, κ_{xy}, which consists entirely of quasiparticles without any phonon background. This is because phonons are scattered symmetrically by the vortices, while there is considerable asymmetry (handedness) in the scattering of quasiparticles as they encounter currents circling around each vortex. The purely quasiparticle nature of κ_{xy} is easily confirmed simply by reversing the magnetic field, which leads to a reversal of the transverse thermal current.

In analogy with a well-known Hall effect relation

$$\sigma_{xy} = \sigma_{xx} \tan\theta_{\mathrm{H}} \tag{15}$$

where θ_{H} is the Hall angle, the transverse and purely electronic (quasiparticles) thermal conductivity, κ_{xy}, is related to the electronic thermal conductivity, κ^{e}_{xx}, according to

$$\kappa_{xy} = \kappa^{\mathrm{e}}_{xx} \tan\theta_R \tag{16}$$

Here we call θ_R the thermal Hall angle. Assuming that the Wiedemann–Franz law applies, θ_R must equal θ_H.

In the geometry of Fig. 4, heat flow imposed along the x-axis in the presence of a magnetic field B_z will give rise to the longitudinal thermal gradient $\nabla_x T$ and the transverse thermal gradient $\nabla_y T$. Using Onsager relations under the condition of zero transverse heat current (no thermal current is injected in the y-direction), and assuming no in-plane anisotropy ($\kappa_{xx} = \kappa_{yy}$), the transverse thermal conductivity, $\kappa_{xy}(H)$ becomes

$$\kappa_{xy}(H) = \kappa_{xx}(H)\frac{\nabla_y T}{\nabla_x T} \tag{17}$$

Thus by measuring the two thermal gradients $\nabla_y T$ and $\nabla_x T$ (or, rather, temperature differences $\Delta_{xx}T$ and $\Delta_{xy}T$ using the thermocouple junctions A and B, and C and D, respectively) and the total field-dependent longitudinal thermal conductivity $\kappa_{xx}(H)$, one can obtain the transverse conductivity $\kappa_{xy}(H)$. Knowing $\kappa_{xy}(H)$—which is due purely to quasiparticles—one can work backward through Eqs. (15) and (16) to determine the longitudinal quasiparticle contribution, κ^{e}_{xx}, and the phonon contribution, $\kappa^{p}_{xx} = \kappa_{xx} - \kappa^{e}_{xx}$.

Although this is a sound experimental approach, caution should be exercised because the Hall angle in the normal state of high-temperature superconductors does not follow the usual relation, $\tan\theta_H = \omega_c\,\tau$, where ω_c is the cyclotron frequency and τ is the transport relaxation time. On the contrary, the behavior of θ_H is highly anomalous. It is likely that this anomalous trend will extend also to temperatures below T_c—that is, the thermal Hall angle of quasiparticles may be anomalous as well. It is thus prudent to determine θ_R independently. By measuring $\kappa_{xy}(H)$ and $\kappa_{xx}(H)$, and taking into account that phonon thermal conductivity in high-temperature superconductors is field independent (as the most recent data seem to indicate), enough information is acquired to determine θ_R independently.

Measurements of transverse thermomagnetic effects are generally challenging, as the magnitude of the signal—the transverse thermal gradient in this case—is quite small, typically on the order of 1 mK/mm even in a field as high as 6 T. The difficulties are compounded by the fact that one does not have available large samples—typical size of high-quality crystals of high-temperature superconductors is not larger than a few millimeters in the basal plane, and perhaps up to one half of a millimeter in thickness. In spite of these limitations, the data clearly reveal exotic characteristics of the superconducting condensate, among them the highly anomalous rise in the relaxation time of quasiparticles below T_c, which is responsible for a substantial fraction of the enhancement in thermal conductivity. Figure 11 summarizes the findings of Krishana et al. (15) obtained on single crystals of $YBa_2Cu_3O_{7-\delta}$.

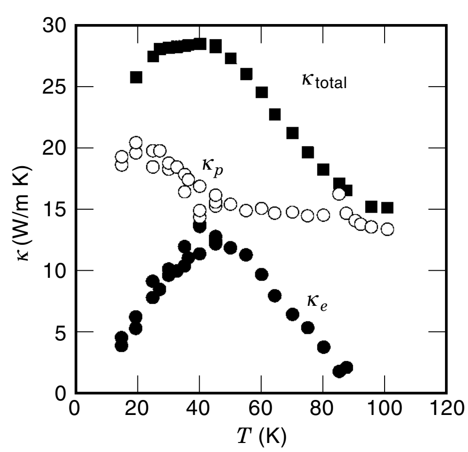

Figure 11. Temperature dependence of thermal conductivity of $YBa_2Cu_3O_7$ below the superconducting transition temperature. Solid squares indicate the total thermal conductivity, open circles are the phonon thermal conductivity contribution, and solid circles are the quasiparticle thermal conductivity. The individual thermal conductivity contributions were obtained from measurements of the Righi–Leduc effect, the thermal equivalent of the Hall effect. Data are from Krishana et al. (15).

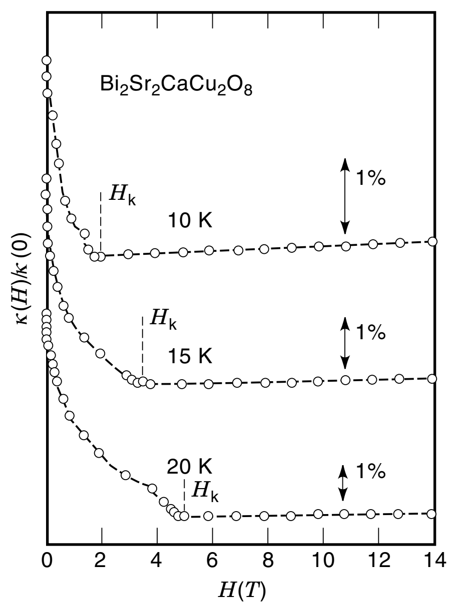

Figure 12. Magnetic field dependence of the thermal conductivity of $Bi_2Sr_2CaCu_2O_8$ at low temperatures. The field dependence disappears sharply above a threshold field H_k, suggestive of a transition in the condensate. At field below H_k, the quasiparticles carry a fraction of the heat current, whereas above H_k, their contribution vanishes. Data are from Krishana et al. (16).

Thermal magnetoresistance has proved to be a powerful probe of superconducting condensates. In addition to solving a puzzle concerning heat transport below T_c, it directly addresses fundamental properties of the superconducting state, such as the symmetry of the gap parameter. Measurements on $Bi_2Sr_2CaCu_2O_8$ in high magnetic fields reveal an entirely unexpected failure of the quasiparticles to conduct heat when the field exceeds a certain strength H_k [see Fig. 12 (16)]. The field H_k delineates two distinct regimes of the condensate: (1) below H_k, where quasiparticles conduct heat and the thermal conductivity decreases with increasing field; and (2) above H_k, where the field dependence of $\kappa(H)$ essentially disappears. The data show the field H_k being strongly temperature dependent, following approximately a quadratic power law dependence.

How can a superconductor suddenly cease to have its thermal conductivity be field dependent? Although other evidence suggests that that the phonon contribution in high-temperature perovskites is field independent, what happens to quasiparticles at H_k that they suddenly ignore the magnetic field? The data suggest that at H_k the condensate undergoes a phase transition to a state in which the quasiparticles not only become field-independent, but the quasiparticle current itself ceases to exist. The field independent thermal conductivity above H_k is then the phonon contribution which, as stated above, is believed to be independent of magnetic field. The measurements provide an additional direct way of assessing the phonon and quasiparticle contributions to the heat current—the latter is simply given by $\kappa_e = \kappa(0, T) - \kappa(H_k, T)$. Furthermore, and fundamentally more important, thermal magnetoresistance reveals a most unusual and completely unexpected phase transition in the condensate taking place at the field H_k. Perhaps this reflects a field-driven change in the symmetry of a gap parameter away from the assumed d-wave symmetry with an ensuing immediate collapse of the quasiparticle population and, hence, an essentially zero electronic thermal conductivity. These exciting issues await further detailed study. It is clear, however, that thermal conductivity, through its field dependence—thermal magnetoresistance—is an exceptionally powerful probe of the superconducting state.

BIBLIOGRAPHY

1. I. A. Smirnov and V. S. Oskotski, in K. A. Gschneider and L. Eyring (eds.), *Handbook on the Physics and Chemistry of Rare Earths,* Vol. 16, New York: Elsevier, 1992, p. 107.
2. P. G. Klemens, Theory of thermal conductivity of solids, in F. Seitz and D. Turnbull (eds.), *Solid State Physics,* New York: Academic Press, 1958.
3. J. M. Ziman, *Electrons and Phonons,* Oxford, UK: Clarendon Press, 1960.
4. J. Mathon, Exchange interactions and giant magnetoresistance in magnetic multilayers, *Contemp. Phys.,* **32**: 143–156, 1991.
5. R. Berman, *Thermal Conduction in Solids,* Oxford, UK: Clarendon Press, 1976.
6. C. Uher, Thermoelectric property measurements, *Nav. Res. Rev.,* **48**: 44–55, 1996.
7. A. Fert and P. Bruno, Interlayer coupling and magnetoresistance in multilayers, in B. Heinrich and J. A. C. Bland (eds.), *Ultrathin Magnetic Structures,* Berlin: Springer-Verlag, 1994.
8. I. A. Campbell and A. Fert, Transport properties of ferromagnets, in E. P. Wohlfarth (ed.), *Ferromagnetic Materials,* Amsterdam: North-Holland, 1982.
9. L. Piraux et al., Magnetothermal transport properties of granular Co-Ag solids, *Phys. Rev.,* **B48**: 638–641, 1993.
10. F. Tsui et al., Heat conduction of (111) Co/Cu superlattices, *J. Appl. Phys.,* **81**: 4586–4588, 1997.
11. Y. Shapira et al., Resistivity and Hall effect of EuSe in fields up to 150 kOe, *Phys. Rev.,* **B10**: 4765–4780, 1974.
12. C. Zener, Interaction between the d-shells in the transition metals. II. Ferromagnetic compounds of manganese with perovskite structure, *Phys. Rev.,* **82**: 403–405, 1951.
13. D. W. Visser, A. P. Ramirez, and M. A. Subramanian, Thermal conductivity of manganite perovskites: Colossal magnetoresistance as a lattice-dynamics transition, *Phys. Rev. Lett.,* **78**: 3947–3950, 1997.
14. C. Uher, Thermal conductivity of high-temperature superconductors, in D. M. Ginsberg (ed.), *Physical Properties of High Temperature Superconductors,* Vol. 3, Singapore: World Scientific, 1992, pp. 159–283.
15. K. Krishana, J. M. Harris, and N. P. Ong, Quasiparticle mean free path in $YBa_2Cu_3O_7$ measured by the thermal Hall conductivity, *Phys. Rev. Lett.,* **75**: 3529–3532, 1995.
16. K. Krishana et al., Plateaus observed in the field profile of thermal conductivity in the superconductor $Bi_2Sr_2CaCu_2O_8$, *Science,* **277** (5322): 82–85, 1997.

CTIRAD UHER
University of Michigan

THERMAL SENSORS. See PYROELECTRICITY.